



## Application of the Mixed $H_2/H_{\infty}$ Method to Design the Microsatellite Attitude Control System

**Erberson Rodrigues Pinheiro, Luiz Carlos Gadelha de Souza.**

Instituto Nacional de Pesquisas Espaciais, INPE,  
Av. dos Astronautas, 1758, 12227-101- São José Dos Campos, SP, Brasil  
gadelha@dem.inpe.br

**Keywords:** *microsatellite, robust control, uncertainty model*

### Abstract

*Due to the space missions' limited budget, small satellite cluster or constellation would be an economical choice. From risk-sharing viewpoint, a number of smaller satellites have a significant reliability advantage over a bigger one. By and large, artificial satellites are subject to two kinds of uncertainty: structure uncertainty that represent some satellite parameter variation and the unstructured uncertainty, which represent some kind of the satellite model error. On the other hand, the Satellite Attitude Control (SAC) design becomes more vulnerable to uncertainty disturbances like model error and moment-of-inertia variation as the satellite has great decrease in size and weight. This is the case for a microsatellite with mass less than 100kg where the ACS performance and robustness becomes very sensitive to both kinds of uncertainties. Therefore, the design of the SAC has to deal with the drawback between controller performance and robustness. The purpose of this work is to model a microsatellite and to perform a mixed Control via LMI optimization.*

### 1 Introduction

Microsatellites play important role in space missions, such as position location, Earth observation, atmospheric data collection, space science and communication. Some spacecraft used to observation need high-accuracy performance on pointing requirement, so it's necessary to apply a three-axis attitude control, leading a multivariable control system [1]. In the face of disturbance and uncertainty, it's necessary to design a robust control for analysis and synthesis of attitude control system. Examples of satellite robust control system design using multi-objective and nonlinear approaches can be found in [2] and [3], respectively. Low orbit spacecraft are under a more strong influence of gravity gradient torque, aerodynamic torque and magnetic torque. Some equipment on the microsatellite like cameras, telescopes and solar array can move causing change on moment of inertia. Microsatellites with mass less than 100kg are more sensitive to moment of inertia variation and disturbances like external torques. In this work will be use a kind of robust control called mixed control. This combination was introduced by Bernstein and Haddad [4], the idea is to minimize a norm of a transfer

function subjected a constraint given by a  $H_\infty$  norm of another transfer function. In the paper [5] was considered state and output-feedback control of the mixed  $H_2/H_\infty$  control and to solve the non-linear Riccati equation was used convex optimization. As for vibration control of rigid-flexible satellite an alternative approach is to use piezoelectric shunt damping technique as has been done in [6]. In this work one uses the mixed  $H_2/H_\infty$  control via the LMI approach [7] to design an attitude control of a microsatellite subjected an external disturbances and uncertainty in the moment of inertia.

## 2 Microsatellite Attitude Dynamics

It is defined a body-fixed reference frame B with its origin located in the center of mass of a microsatellite and is given the unit vectors being along the principal axes. The Euler's equations of a microsatellite is given by [8]

$$\begin{aligned} I_x \dot{\omega}_x - (I_y - I_z) \omega_y \omega_z &= T_{ex} + T_{gx} + u_x, \\ I_y \dot{\omega}_y - (I_z - I_x) \omega_z \omega_x &= T_{ey} + T_{gy} + u_y, \\ I_z \dot{\omega}_z - (I_x - I_y) \omega_x \omega_y &= T_{ez} + T_{gz} + u_z, \end{aligned} \quad (1)$$

where  $I_x$ ,  $I_y$  and  $I_z$  are the principal moments of inertia,  $\omega_x$ ,  $\omega_y$  and  $\omega_z$  are the body-axis components of angular velocity,  $T_{ex}$ ,  $T_{ey}$  and  $T_{ez}$  are the no modelled external torques,  $T_{gx}$ ,  $T_{gy}$  and  $T_{gz}$  are the components of gravity gradient torques that will be inserted into the equations and  $u_x$ ,  $u_y$  and  $u_z$  are the control torques.

It's necessary to consider another reference system, called local-vertical-local-horizontal (LVLH) with its origin at the center of mass of the microsatellite. The LVLH frame has the following unitary vectors  $\{a_1, a_2, a_3\}$ , with  $a_1$  in the direction of the microsatellite velocity in the orbital plane,  $a_3$  pointing to the Earth, and  $a_2$  normal to the orbit plane.

To describe the orientation of the body-fixed frame B with respect of LVLH frame in terms of Euler angles, is used the following coordinate transformation

$$\begin{bmatrix} \mathbf{i} \\ \mathbf{j} \\ \mathbf{k} \end{bmatrix} = \begin{bmatrix} c\theta c\psi & c\theta s\psi & -s\theta \\ s\phi s\theta c\psi - c\phi s\psi & s\phi s\theta s\psi + c\phi c\psi & s\phi c\theta \\ c\phi s\theta c\psi + s\phi s\psi & c\phi s\theta s\psi - s\phi c\psi & c\phi c\theta \end{bmatrix} \begin{bmatrix} \mathbf{a}_1 \\ \mathbf{a}_2 \\ \mathbf{a}_3 \end{bmatrix}. \quad (2)$$

The angular velocity of the body fixed frame B relative to the LVLH is given by

$$\vec{\omega}^{B/A} = \omega_x^{B/A} \mathbf{i} + \omega_y^{B/A} \mathbf{j} + \omega_z^{B/A} \mathbf{k}, \quad (3)$$

where

$$\begin{bmatrix} \omega_x^{B/A} \\ \omega_y^{B/A} \\ \omega_z^{B/A} \end{bmatrix} = \begin{bmatrix} 1 & 0 & -s\theta \\ 0 & c\phi & s\phi c\theta \\ 0 & -s\phi & c\phi c\theta \end{bmatrix} \begin{bmatrix} \dot{\phi} \\ \dot{\theta} \\ \dot{\psi} \end{bmatrix}. \quad (4)$$

The angular velocity of the body fixed frame B relative to the inertial frame N fixed in the Earth center becomes

$$\vec{\omega} = \vec{\omega}^{B/N} = \vec{\omega}^{B/A} + \vec{\omega}^{A/N} = \vec{\omega}^{B/A} - n \vec{a}_2 \quad (5)$$

where

$$\begin{bmatrix} \omega_x \\ \omega_y \\ \omega_z \end{bmatrix} = \begin{bmatrix} 1 & 0 & -s\theta \\ 0 & c\phi & s\phi c\theta \\ 0 & -s\phi & c\phi c\theta \end{bmatrix} \begin{bmatrix} \dot{\phi} \\ \dot{\theta} \\ \dot{\psi} \end{bmatrix} - n \begin{bmatrix} c\theta s\psi \\ s\phi s\theta s\psi + c\phi c\psi \\ c\phi s\theta s\psi - s\phi c\psi \end{bmatrix}. \quad (6)$$

$n$  is the orbital frequency of the microsatellite.

For small attitude deviation from LVLH orientation, the following linearized attitude dynamics can be obtained

$$\begin{aligned} \omega_x &= \dot{\phi} - n\psi, \\ \omega_y &= \dot{\theta} - n, \\ \omega_z &= \dot{\psi} + n\phi \end{aligned} \quad (7)$$

### 2.1 Gravity Gradient Torque

In the space, the gravitational field is not uniform, so the variation in the gravitational field over the body yields the gravitational torque about of the center of mass of the body. On the assumption that the microsatellite center of mass is in a Keplerian circular orbit and the Earth is spherical, the gravity gradient torque along the body axes become

$$\begin{aligned} T_{gx} &= 3n^2(I_z - I_y)\phi, \\ T_{gy} &= 3n^2(I_z - I_x)\theta, \\ T_{gz} &= 0. \end{aligned} \quad (8)$$

Inserting the gravity gradient equations (8) into the Euler equations (1) and making a linearization, one has

$$\begin{aligned} I_x\ddot{\phi} - n(I_x - I_y + I_z)\dot{\psi} + 4n^2(I_y - I_z)\phi &= T_{ex} + u_x, \\ I_y\ddot{\theta} + 3n^2(I_x - I_z)\theta &= T_{e2} + u_y, \\ I_z\ddot{\psi} + n(I_x - I_y + I_z)\dot{\phi} + n^2(I_y - I_x)\psi &= T_{e3} + u_z. \end{aligned} \quad (9)$$

These equations are the Euler equations for the microsatellite, from which one observes that the pitch axis is decoupled from the roll and yaw axes.

### 3 Structured uncertainty

To represent the system uncertainty  $\Delta$  it will be used Linear Fractional Transformation (LFT) [9]. As showed in Figure 1, using the LFT procedure the block transfer function from the perturbation signal  $w$  to error signal  $z$  is given by

$$z = [M_{22} + M_{21}\Delta(I - M_{11}\Delta)^{-1}M_{12}]\omega, \quad (10)$$

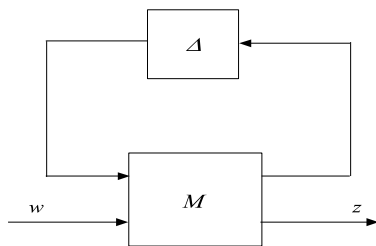


Figure 1. Uncertainty representation in LFT block diagram

The plant of the system can be represented by the block M which is given by

$$M = \begin{bmatrix} M_{11} & M_{12} \\ M_{21} & M_{22} \end{bmatrix}, \quad (11)$$

Considering that there is uncertainty in the principal moment of inertia of the microsatellite,

it can be expressed as a nominal value plus a perturbation [7] given by

$$I_i = \bar{I}_i + p_i\delta_i, \quad i = 1,2,3, \quad (12)$$

where  $p_i$  is the variation and  $\delta_i$  the normalized uncertainty. Inserting it into the Euler equations, one has the dynamic equation with uncertainty. This uncertainty can be pulled out of the system and it can be considered like a disturbance.

Let's do this calculation, initially, for pitch axis of the microsatellite which is decouple,  $d$  is the disturbing torque. As result, the equation of motion is given by

$$I_y\ddot{\theta} + 3n^2(I_x - I_z)\theta = u_y + d, \quad (13)$$

This equation of motion can be put in the block diagram as showed by Figure 2.

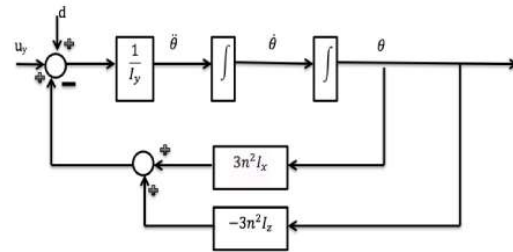


Figure 2. Block diagram of the pitch axis.

Using the Linear Fractional Transformation (LFT), the first block of the Figure 2 can be represented by

$$\begin{aligned} \frac{1}{I_y} &= \frac{1}{\bar{I}_y + p_y\delta_y}, \\ &= \frac{1}{\bar{I}_y} - \frac{p_y}{\bar{I}_y} \delta_y \left(1 + \frac{1}{\bar{I}_y} \delta_y\right)^{-1} \frac{1}{\bar{I}_y}, \end{aligned} \quad (14)$$

Comparing this equation with the LFT Equation (11) the first block will be

$$M_1 = \begin{bmatrix} -\frac{p_y}{\bar{I}_y} & \frac{1}{\bar{I}_y} \\ -\frac{p_y}{\bar{I}_y} & \frac{1}{\bar{I}_y} \end{bmatrix}. \quad (15)$$

Doing the same procedure for the second and the third block are given by

$$3n^2 I_x = 3n^2(\bar{I}_x + p_x \delta_x),$$

$$M_2 = \begin{bmatrix} 0 & 1 \\ 3n^2 p_x & 3n^2 \bar{I}_x \end{bmatrix}, \quad (16)$$

$$3n^2 I_z = 3n^2(\bar{I}_z + p_z \delta_z),$$

$$M_3 = \begin{bmatrix} 0 & -1 \\ 3n^2 p_z & -3n^2 \bar{I}_z \end{bmatrix} \quad (17)$$

As a result, the new block diagram for the pitch axis taking into account the uncertainty is as showed in Figure 3.

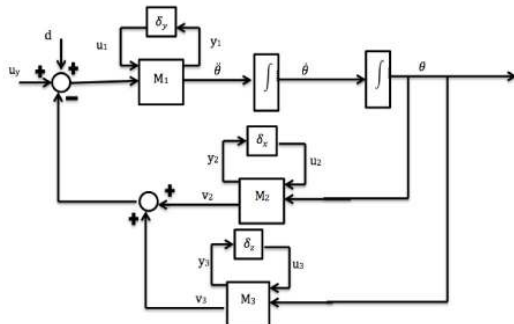


Figure 3. Pitch axis block diagram with uncertainty.

This representation helps to understand how the uncertainty acts in the system and how it can be lumped out of the system like a perturbation. Usually, the uncertainty is incorporated in the generalized plant in the diagonal form as it will be showed later.

The mixed design H<sub>2</sub>/H<sub>∞</sub> approach [5] consist, initially, minimizing the perturbation effect of moment of inertia uncertainty (structured) by the H<sub>∞</sub> norm. On the other hand, the external disturbance uncertainty (unstructured) will be minimized by the H<sub>2</sub> norm. As a result, the closed loop system remains stable for external perturbation, which is associated with good performance, for example, quick time response and small overshoot.

In order to include both kinds of uncertainties so as the controller designed presents good

robustness and adequate performance the new generalized plant must has both signals that will be minimized. Here the generalized plant in matrix form is given by

$$\begin{bmatrix} \dot{\theta} \\ \ddot{\theta} \\ z_{\infty} \\ z_2 \\ y \end{bmatrix} = \begin{bmatrix} 0 & 1 & 0 & 0 & 0 & 0 & 0 \\ \frac{-3n^2(I_x - I_z)}{I_y} & 0 & -\frac{p_y}{I_y} & -\frac{3n^2 p_x}{I_y} & -\frac{3n^2 p_z}{I_y} & -\frac{1}{I_y} & -\frac{1}{I_y} \\ \frac{-3n^2(I_x - I_z)}{I_y} & 0 & -\frac{p_y}{I_y} & -\frac{3n^2 p_x}{I_y} & -\frac{3n^2 p_z}{I_y} & -\frac{1}{I_y} & -\frac{1}{I_y} \\ 1 & 0 & 0 & 0 & 0 & 0 & 0 \\ -1 & 0 & 0 & 0 & 0 & 0 & 0 \\ Q_1 & 0 & 0 & 0 & 0 & 0 & 0 \\ 0 & Q_2 & 0 & 0 & 0 & 0 & 0 \\ 0 & 0 & 0 & 0 & 0 & 0 & R \\ 1 & 0 & 0 & 0 & 0 & 0 & 0 \end{bmatrix} \begin{bmatrix} \theta \\ \dot{\theta} \\ u_1 \\ u_2 \\ u_3 \\ d \\ u \end{bmatrix} \quad (18)$$

In that case, one has the inputs (u1, u2, u3, u), the outputs (z<sub>∞</sub>, z<sub>2</sub>, y), the state's x (θ, dθ/dt) and the perturbation d=w. As a result, the new state space model that include both kinds of design requirements is given by

$$\begin{aligned} \dot{x} &= Ax + B_1 w + B_2 u, \\ z_{\infty} &= C_1 x + D_{11} w + D_{12} u. \\ z_2 &= C_2 x + D_{22} u. \end{aligned} \quad (19)$$

As a result, the generalized plant P is given by

$$P = \begin{bmatrix} A & B_1 & B_2 \\ C_1 & D_{11} & D_{12} \\ C_2 & D_{21} & D_{22} \end{bmatrix}, \quad (20)$$

#### 4 The Mixed H<sub>2</sub>/H<sub>∞</sub> Controller Theory

Figure 4 shows the block diagram of the mixed H<sub>2</sub>/H<sub>∞</sub> control approach [5], where the above block represents the uncertainty, the medium block is the generalized plant and the below block is the controller to designed.

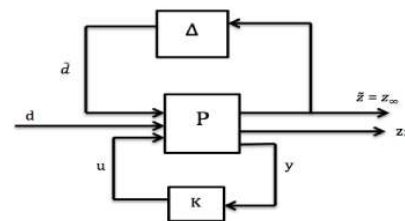


Figure 4. Block diagram of the general configuration.

As showed in [7] the mixed  $H_2/H_\infty$  control problem is equivalent to minimize Trace  $T_r(Q)$  over the matrices  $X=X^T$ ,  $Q=Q^T$  and  $Y$  satisfying the Linear Matrix Inequalities [9] given by

$$\begin{bmatrix} AX - B_2 + (AX - B_2Y)^T & B_1 & (C_1X - D_{12}Y)^T \\ B_1^T & -I & D_{11}^T \\ C_1X - D_{12}Y & D_{11} & \gamma^2 I \end{bmatrix} < 0,$$

$$\begin{bmatrix} Q & C_2X - D_{22}Y \\ (C_2X - D_{22}Y)^T & X \end{bmatrix} > 0.$$

Assuming that the LMIs above equations have solutions  $Y^*$ ,  $X^*$ ,  $Q^*$ , the mixed  $H_2/H_\infty$  controller  $K^*$  is given by

$$K^* = Y^*(X^*)^{-1} \quad (21)$$

As a result, the mixed  $H_2/H_\infty$  controller design is a multi-objective control problem where the goal is to minimize the  $H_2$  norm in order to improve performance subjected to the minimization of  $H_\infty$  norm to guaranty robustness requirement [9], which results in the two following expressions

$$\text{Min. } \|T_{z_2w}\|_2 \leq \sqrt{\text{trace}(Q^*)} \quad (22)$$

$$\text{Subject } \|T_{z_\infty w}\|_\infty = \gamma \quad (23)$$

#### 4 Simulations and Results

The microsatellite used in the simulation has inertia moment  $I_x = 18.4 \text{ Kg m}^2$ ,  $I_y = 18.2 \text{ Kg m}^2$ ,  $I_z = 6.8 \text{ Kg m}^2$ , its mass  $m = 60 \text{ Kg}$  and dimension =  $50 \times 50 \times 60 \text{ cm}$ . In the simulations, the initial attitude in roll, pitch, yaw are  $(10, 10, 10)$  degree and the initial angular velocity in roll, pitch, yaw are  $(0.6, 0.6, 0.6)$  degree/s.

In the mixed  $H_2/H_\infty$  controller design a key point is to find the appropriate values of  $\gamma$ . Besides, one must keep in mind that for  $\gamma = \gamma_{min}$  one has the pure  $H_\infty$  control problem and  $\gamma = \gamma_{max}$  one has the pure  $H_2$  control problem. Here, just for simulations propose one decides to begin using  $\gamma = 2$  to perform a comparative study.

As for the uncertainty, one assumes that the variation on the moment of inertia is about 10%. In order to obtain the maximum and the minimum uncertainty variations, one considers two kind of plant, given by:

Plant with uncertainty 1:  $\Delta I_x = +10\%I_x$ ,  
 $\Delta I_y = -10\%I_y$  and  $\Delta I_z = -10\%I_z$

Plant with uncertainty 2:  $\Delta I_x = -10\%I_x$ ,  
 $\Delta I_y = +10\%I_y$  and  $\Delta I_z = +10\%I_z$

Figure 5 shows the Euler angle of roll, pitch and yaw with uncertainty, where the dashed line represents the plant with uncertainty variation and the continuous line the nominal plant without uncertainty. One can see that for pure  $H_\infty$  control ( $\gamma = \gamma_{min} = 0.2$  - blue line) the controller is very robust with respect to uncertainty, because there is no difference between the nominal plant and the plant with uncertainty. On the other hand, it's noted that difference between the nominal plant and the plant with uncertainty increase for pure  $H_2$  control ( $\gamma = \gamma_{max} = 100$  - red line).

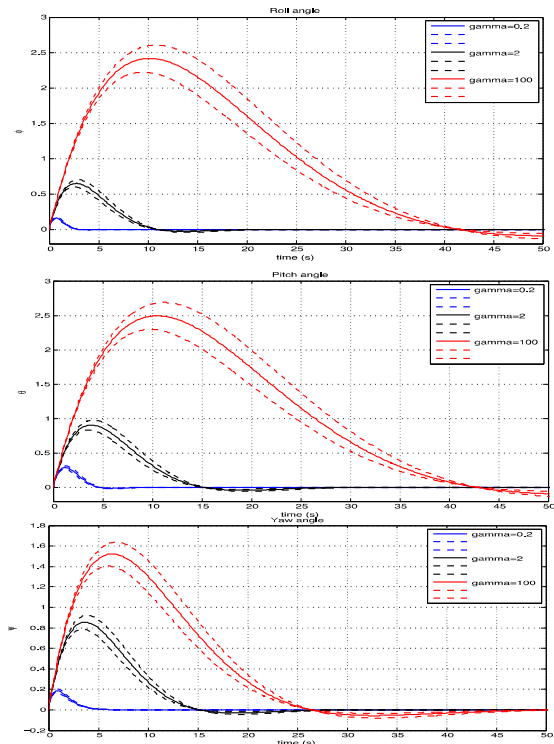


Figure 5. The mixed  $H_2/H_\infty$  controller for Euler angle of roll, pitch and yaw with uncertainty.

Figure 6 shows the mixed  $H_2/H_\infty$  controller signal for roll, pitch and yaw axes, where for pure  $H_\infty$  control (blue line), the controller signal has bigger overshoot than for pure  $H_2$  control (red line), which represents the drawback between its robustness and performance. Considering that the microsatellite actuator must have small torque the mixed  $H_2/H_\infty$  control with  $\gamma = 2$  is a good choice to design the controller, because it is not so slow like pure  $H_2$  and the control signal is not so strong like pure  $H_\infty$  control.

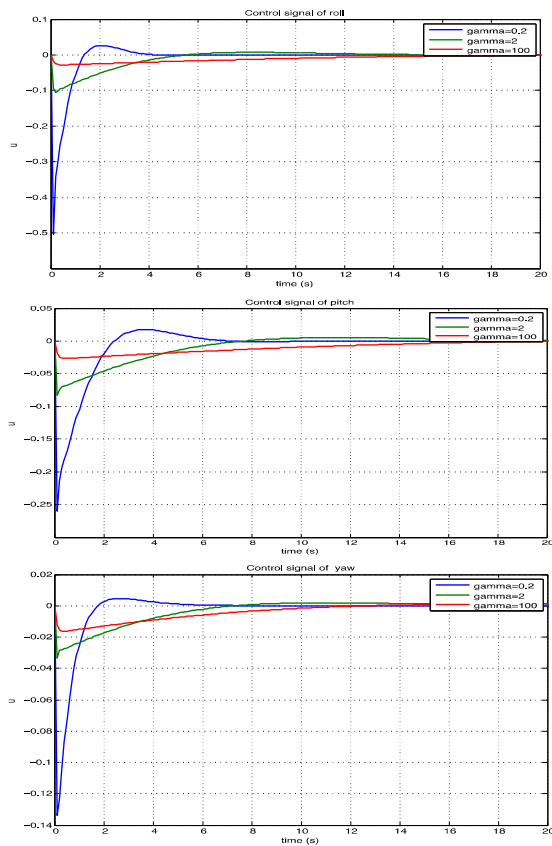


Figure 6 – The mixed  $H_2/H_\infty$  controller signal for the roll, pitch and yaw axes

Spacecraft is subjected to small disturbances on the space, and these disturbances can be persistent. In the case of a low orbit the microsatellite is more subject to disturbances due to the gravity gradient, magnetic and aerodynamic torques. The gravity gradient torque is included into the equations, the magnetic torque is cyclic and can be

approximated by sinusoids with different frequencies and the aerodynamic torque is cumulative and can be approximated to a step. As result, one has assume that these torque can be represented by the following equation [8]

$$T_{ext} = \sum_k 10^{-5} \sin(knt) + 3 \times 10^{-5} [\sigma(t - 1000) - \sigma(t - 4000)] \quad (24)$$

Figure 7 shows the Euler angles (roll, pitch, yaw) for pure  $H_\infty$  control (blue line), the mixed control  $H_2/H_\infty$  ( $\gamma = 2$  – black line) and the pure  $H_2$  control (red line). One observes that the pure  $H_\infty$  control has the best capacity of attenuation with respect to a sinusoidal disturbance. The pure  $H_2$  control is not robust with respect to a sinusoidal disturbance. In order to have a good balance control between robustness and performance it's necessary choose some values of  $\gamma$  such that the mixed control  $H_2/H_\infty$  provide a good performance even with the perturbation of the external torques. Again the best mixed control  $H_2/H_\infty$  controller value for  $\gamma$  is 2.

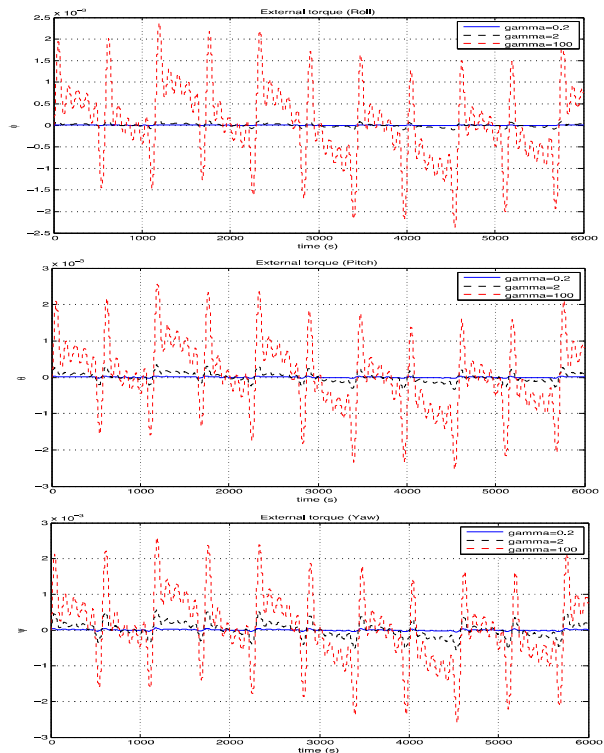


Figure 7. The mixed  $H_2/H_\infty$  controller response to external torques for roll, pitch and yaw axes.

## 5 Conclusion

This paper presents a microsatellite model taking into account the uncertainties and the design of the satellite control system based on the mixed  $H_2/H_\infty$  methodology via LMI optimization. This control technique is used to design the microsatellite attitude control system in the face of environmental disturbance (unstructured uncertainty) and moment of inertia variation (structured uncertainty). It is well known that the  $H_\infty$  controller provides robust stability with respect to structured uncertainty while the  $H_2$  controller provides good performance with a respect to unstructured uncertainty. Here, one investigates the conjunction of the both methods in order to improve the performance and robustness of the SAC system. To do this, one assumes that the microsatellite is subjected to uncertainty in the moment of inertia variation of about 10% and environmental disturbances were approximated to sinusoidal function plus a step function. The simulations have shown that the  $H_\infty$  controller has presented best robustness and performance than the  $H_2$  controller with respect to uncertainty due to inertia moment variation and due external disturbance. However, in all simulations the  $H_\infty$  controller signal was bigger than the  $H_2$  controller, which can cause bigger overshoot and can saturate the actuator, once microsatellite usually need small actuator. As a result, the way to achieve robustness stability and good performance was to design the controller using the mixed  $H_2/H_\infty$  control, because in this procedure one can choose an adequate value for the tuning parameter  $\gamma$  so as one can have robust control and with low control signal.

## Referencies

- [1] Cubillos, X. C. M. ; Souza, L. C. G. Using of H-Infinity Control Method in Attitude Control System of Rigid-Flexible Satellite. *Mathematical Problems in Engineering*, v. 2009, p. 1-10, 2009.
- [2] Mainenti, I ; Souza, L. C. G. ; Souza, F L . Design of a nonlinear controller for a rigid-flexible satellite using multi-objective Generalized Extremal Optimization with real codification. *Shock and Vibration*, v. 19, p. 1-10, 2012.

- [3] Souza, L. C. G. ; Gonzalez, R G. Application of the state-dependent Riccati equation and Kalman filter techniques to the design of a satellite control system. *Shock and Vibration*, v. 19, p. 22-28, 2012.
- [4] D. S. Bernstein. and W. M. Haddad, LQG control with an  $H_\infty$  performance bound: A Riccati equation approach. *IEEE Transactions on Automatic Control*, 34(3), 293–305, 1989.
- [5] P. P. Khargonekar and M. A. Rotea, Mixed  $H_2/H_\infty$  control: A convex optimization approach. *IEEE Transactions on Automatic Control*, 36(7), 824–837, 1991.
- [6] Sales, T.P. ; Rade, D.A. ; Souza, L.C.G. . Passive vibration control of flexible spacecraft using shunted piezoelectric transducers. *Aerospace Science and Technology*, v. 1, p. 12-26, 2013.
- [7] C. Yanga and P. Sun, Mixed  $H_2/H_\infty$  state-feedback design for microsatellite attitude control, *Control Engineering Practice*, Vol 10, pp. 951–970, 2002.
- [8] J. R. Wertz and W.J. Larson, *Space Mission Analysis and Design*, Microcosm Press, California. 1989.
- [9] S. Boyd, L. El Ghaoui, E. Feron, V. Balakrishnan, *Linear matrix inequalities in system and control theory*, SIAM studies in applied mathematics. Philadelphia, PA: SIAM. 1994.